University of Birmingham Lab Report

Pages 1–4
2024

The Validity of the Grazing Angle Method for Determining Radiation Damage

Elliott Pritchard Wright
MSci Physics
School of Physics and Astronomy
7 August 2024

Keywords: keyword1, keyword2, keyword3, etc.

ABSTRACT

1 INTRODUCTION

This report concerns the testing of the validity of the grazing angle method in determining the radiation damage on a depleted monolithic active pixel sensor (DMAPS). In this investigation, the DMAPS is MALTA2. A test beam of protons impinges on a telescope of 7 MALTA2 sensors. An analysis of the mean cluster size against the fourth detector's rotation is conducted and compared with experimentally measured values for an equivalent set-up with 1×10^{15} 1 MeV n_{eq}/cm^2 irradiated detectors.

2 LHC-HL PHYSICS

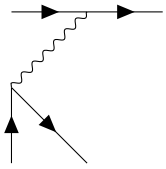

3 RADIATION DAMAGE

4 MALTA2

As previously mentioned, MALTA2 is a DMAPS, which means all of its readout electronics are embedded on the same layer of the PCB as the sensor itself. It was first developed at the end of 2020, following the submission of MALTA and miniMALTA in 2018 and 2019 respectively [1]. MALTA2's layout follows Table 1 and Fig. 1

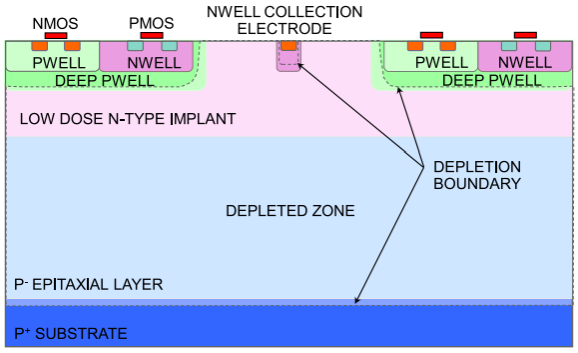

Fig. 1. MALTA layout [1]

Parameter	Value
Sensor Dimension	20.2 mm x 10.1168 mm
Pixel Pitch	36.4 μm x 36.4 μm
Pixel Matrix	512 x 224
Sensor Thickness	100 μm
Sensor Excess	0.7816 mm x 0.9812 mm

Table 1. Table of sensor parameters

5 ALLPIX SQUARED

Allpix Squared is a Monte Carlo simulation software based on Geant4.

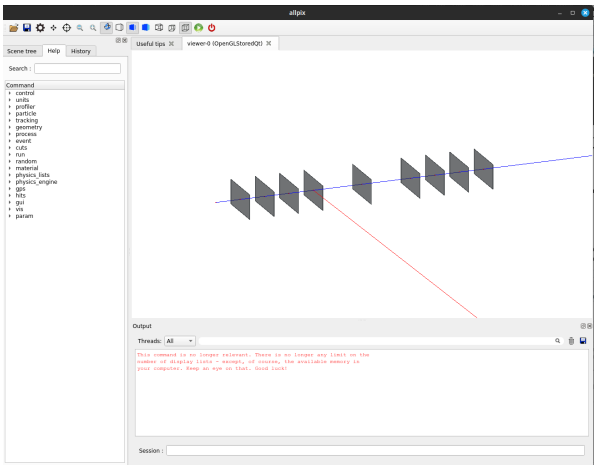

Fig. 2. Allpix Squared simulation visualization where the blue line represents the beam line. Each of the grey rectangles are the MALTA2 sensors.

6 CONSTRUCTING A SENSOR TEST BEAM SIMULATION

To begin with, we took the alpide model from the featured Allpix models and changed the relevant parameters to match those in Table 1. Then we created a detector configuration file, specifying the alpide as the detector type, and arranging the 7 detectors/sensors as per Table 2. The operational parameters in Table 3 represent the conditions used in the experimental equivalent to this Monte Carlo simulation.

Z-axis position (mm)
0
80
160
550
940
1020
1100

Table 2. Sensor z-axis positions

Parameter	Value
Particle	Proton
Energy	180GeV
Temperature	258.15K
Depletion Voltage	-30V
Digitisation Threshold	260e

Table 3. Simulation operational parameters

For the simulation constructed, a linear electric field is used, as per the equation below,

$$E(z) = \frac{|U_{bias}| - |U_{depl}|}{d} + 2\frac{|U_{depl}|}{d}\left(1 - \frac{z}{d}\right). \quad (1)$$

When initialising the simulation, it's worth noting that detector geometries are generated equally in the positive and negative x- and y-axis respectively. This meant that the beam must be initialised at the world origin point solely on the z-axis.

7 AUTOMATING THE ALLPIX SIMULATION PROCESS

Due to the inefficient nature of collecting mean cluster sizes for angles from 0 - 60 degrees in 5-degree increments for each of the bias voltages, it was decided the process should be automated. To do this, the generated Python program started by updating the detector configuration file with the correct angle. It then executed the full configuration file, saved the outputted ROOT file, and extracted the mean and standard deviation for the x and y cluster sizes. These steps repeated for 0 - 60 degrees in 5-degree increments, and then all the data was saved to a CSV.

8 COMPARING CLUSTER SIZES

8.1 Method

Data was taken for $V_{bias} = -6V, -9V, -15V, -20V, -25V,$ and $-30V$ with $V_{depletion} = -30V$. Plots of the average cluster size and depletion depth against the incident angle and bias voltage respectively were made. These plots should demonstrate a linear relationship according to the grazing angle method, depicted in Fig. 3.

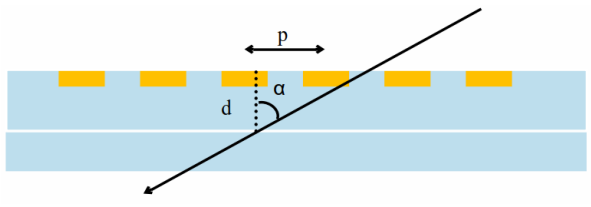

Fig. 3. Grazing angle diagram

From this figure, the cluster size at a given angle α should follow,

$$Cluster(\tan(\alpha)) = \frac{d}{p}\tan(\alpha) + Cluster(0), \quad (2)$$

where d is the depletion depth and p is the pixel pitch. To investigate the conformity of this further, a first-order fit was applied to the cluster data for $\tan(\theta) > 0.5$. The gradient of this was multiplied by the pixel pitch to give the depletion depth for each bias voltage. Once the first-order fit is taken for the cluster data, it was compared to the depletion width

$$w_d = \sqrt{\frac{2\epsilon(V_b + V_{bi})}{Ne}}, \quad (3)$$

where V_b and V_{bi} are the bias and built-in voltage respectively. For the detector under consideration, it is assumed that $V_b \gg V_{bi}$ and therefore

$$w_d \propto \sqrt{V_b}. \quad (4)$$

8.2 Results

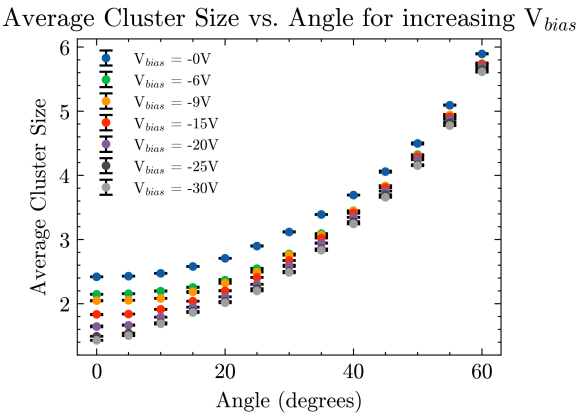

Fig. 4. Average cluster size vs. Angle for increasing bias voltages.

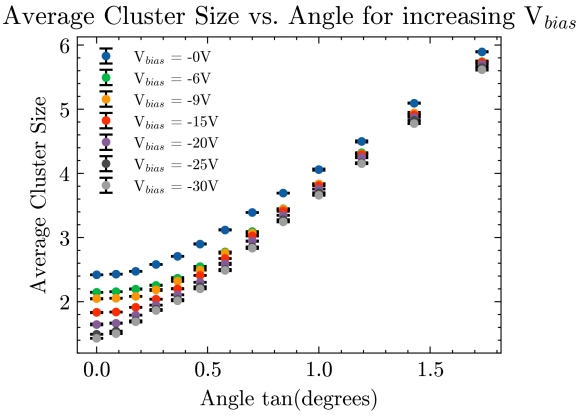

Fig. 5. Average cluster size vs. tan(angle) for increasing bias voltage. This should demonstrate a linear relationship, as per the equation above. This is only seen for $\tan(\text{angle}) > 0.5$.

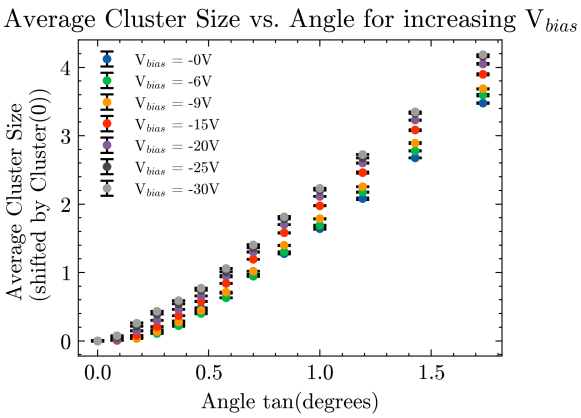

Fig. 6. Average cluster size vs. Angle for increasing bias voltages. This data is taken from the same run as the previous figure but shifted by Cluster(0).

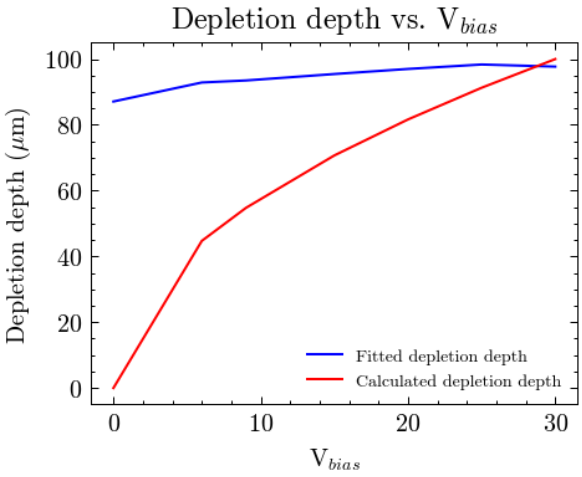

Fig. 7. Depletion depth vs. bias voltage for the linearly fitted data in the figure above (blue), and calculated for the depletion width equation. The full MALTA2 telescope is used when taking this data.

8.3 Analysis

Investigating Fig. **??**sizefig:tan$_c luster_sizeanbeseenthatlinearitycanonlybeas$ 0.5. The cluster size at zero degrees also decreases with increasing bias voltage. In Fig. 7 the fitted and calculated data do not match over the complete run of bias voltages.

9 INVESTIGATING ELECTRON-HOLE DIFFUSION

9.1 Method

In the previous investigation, we saw that at increasing bias voltages, the cluster size at zero degrees decreases. This suggests that the increasing electric field decreases the proportion of charge sharing occurring between pixels. To characterise this fully, we must look at the electron-hole diffusion. Allpix has a built-in way to see the electron diffusion in the sensor via line graphs, as in the figures below.

9.2 Results

9.3 Analysis

We can see that when the telescope is removed, less scattering occurs before the proton beam enters the DUT. When looking at the hitmap for

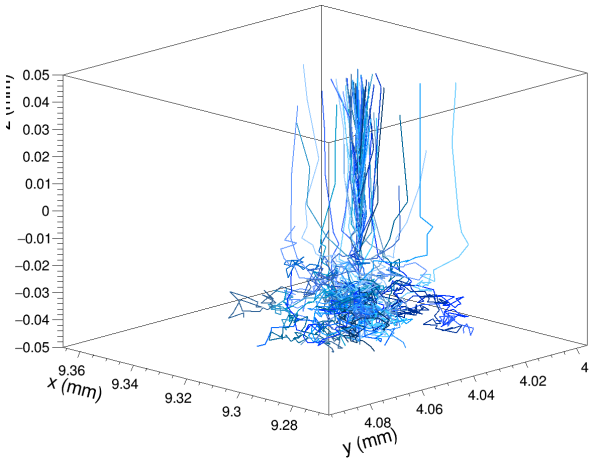

Fig. 8. 3D demonstration of electron drift and diffusion in MALTA2 DUT sensor at 0 degrees incline. A full depletion voltage of -30V is used and -15V bias.

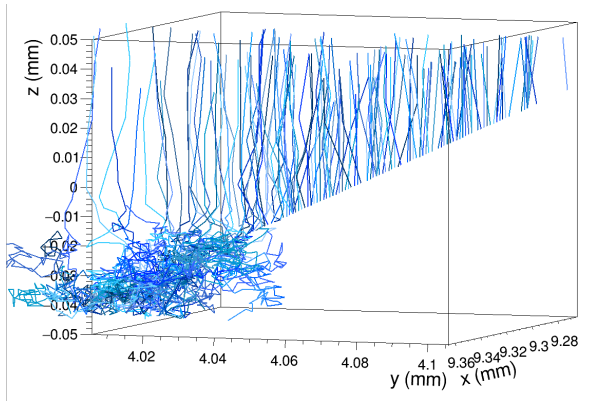

Fig. 9. 3D demonstration of electron drift and diffusion in MALTA2 DUT sensor at 60 degrees incline. A full depletion voltage of -30V is used and -15V bias.

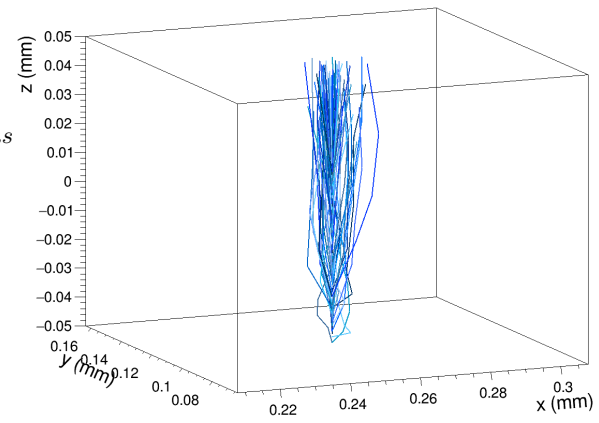

Fig. 10. Drift and diffusion of electrons in MALTA2 DUT sensor at 0 degree incline without the telescope. A full depletion voltage of -30V is used and -30V bias.

the fully depleted sensor, scratches are observed which correspond to electrons scattered in the sensor material before reaching the collection electrode. These are then minimized when the detector is overbiased at $V_{bias} = -50V$ for the 0 degree measurement, but not for the 60 degree

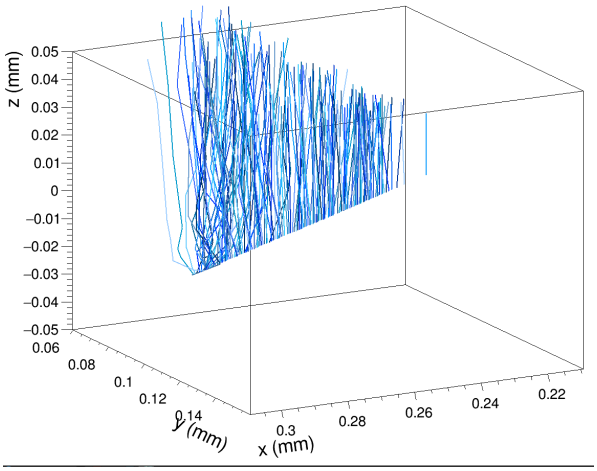

Fig. 11. Drift and diffusion of electrons in MALTA2 DUT sensor at 60 degree incline without the telescope. A full depletion voltage of -30V is used and -30V bias.

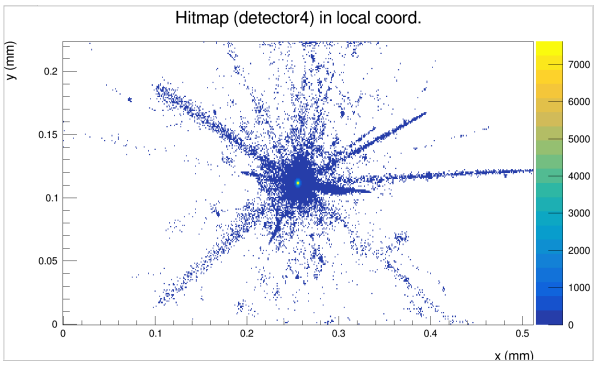

Fig. 12. Hitmap for pixels in the MALTA2 DUT sensor at 0 degrees incline without the telescope. A full depletion voltage of -30V is used and -30V bias.

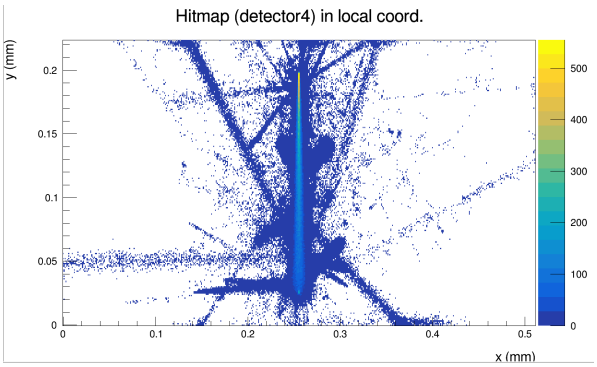

Fig. 13. Hitmap for pixels in the MALTA2 DUT sensor at 60 degrees incline without the telescope. A full depletion voltage of -30V is used and -30V bias.

measurement. This therefore explains the decreased 0 degree cluster size as the stronger electric field minimizes charge sharing.

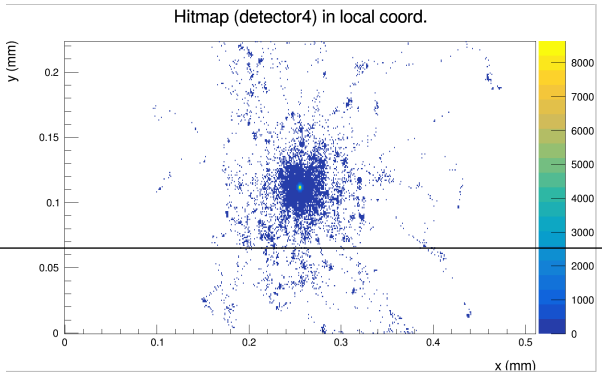

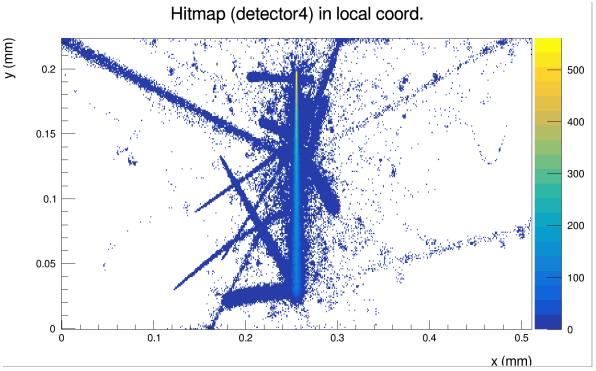

Fig. 15. Hitmap for pixels in the MALTA2 DUT sensor at 60 degrees incline without the telescope. A full depletion voltage of -30V is used and -50V bias.

10 INVESTIGATING THE EFFECT OF DIFFUSION

Due to the scratches seen in the figures above, an investigation was conducted into the effect of diffusion on their size. It was discovered that the width of the depletion region follows

The cut-off for the electric field occurs at w_d. For the investigation

$\|V_{bias}\|$	Calculated	Actual
...	...	...
...	...	...
...	...	...
...	...	...
...	...	...
...	...	...

Table 4. Table of the bias voltage compared the calculated and actual depletion width.

REFERENCES

[1]C. Solans Sánchez et al. Malta monolithic pixel sensors in towerjazz 180 nm technology. *Nuclear Instruments and Methods in Physics Research Section A: Accelerators, Spectrometers, Detectors and Associated Equipment*, 1057:168787, 2023.